



n -level output space mapping for electromagnetic design optimization

Ramzi Ben Ayed, Stephane Brisset

► To cite this version:

Ramzi Ben Ayed, Stephane Brisset. n -level output space mapping for electromagnetic design optimization. COMPEL: The International Journal for Computation and Mathematics in Electrical and Electronic Engineering, 2014, 33 (3), pp.868 - 878. <10.1108/compel-10-2012-0222>. <hal-01913941>

HAL Id: hal-01913941

<https://hal.science/hal-01913941v1>

Submitted on 21 Nov 2018

HAL is a multi-disciplinary open access archive for the deposit and dissemination of scientific research documents, whether they are published or not. The documents may come from teaching and research institutions in France or abroad, or from public or private research centers.

L'archive ouverte pluridisciplinaire **HAL**, est destinée au dépôt et à la diffusion de documents scientifiques de niveau recherche, publiés ou non, émanant des établissements d'enseignement et de recherche français ou étrangers, des laboratoires publics ou privés.



HAL Authorization

***n*-LEVEL OUTPUT SPACE MAPPING FOR ELECTROMAGNETIC DESIGN OPTIMIZATION**

Ramzi BEN AYED, Stéphane BRISSET

Univ Lille Nord de France, F-59000 Lille, France
ECLille, L2EP, F-59650 Villeneuve d'Ascq, France

Abstract.

Purpose – The aim of this paper is to reduce the evaluation number of the fine model within the output space mapping technique in order to reduce their computing time.

Design/methodology/approach –In this paper, *n*-level output space mapping is proposed and expected to be even faster than the conventional output space mapping. The proposed algorithm takes advantages of the availability of *n* models of the device to optimize, each of them representing an optimal trade-off between the model error and its computation time. Models with intermediate characteristics between the coarse and fine models are inserted within the proposed algorithm to reduce the number of evaluations of the consuming time model and, then the computing time. The advantages of the algorithm are highlighted on the optimization problem of superconducting magnetic energy storage.

Findings – A major computing time gain equals to 3 is achieved using the *n*-level output space mapping algorithm instead of the conventional output space mapping technique on the optimization problem of superconducting magnetic energy storage.

Originality/value – The originality of this paper is to investigate several models with different granularities within output space mapping algorithm in order to reduce its computing time without decreasing the performance of the conventional strategy.

Keywords: Finite element model, Optimization, Output Space Mapping, Superconducting Magnetic Energy Storage.

I- INTRODUCTION

In electrical engineering field, space mapping (SM) techniques (Echeverria *et al.*, 2005) and (Bandler *et al.*, 1994) are recognized as iterative optimization strategies that avoid the use of a computationally expensive (fine) model in the optimization process by shifting the optimization burden from the fine model to a cheap (coarse) one. Generally speaking, the coarse model means a low fidelity model which can be evaluated in a very short time and the fine model is an accurate model which consumes computing time.

In each iteration of SM a surrogate model is constructed from the coarse model in such a way that each constructed one is a suitable distortion of the cheap model, such that given matching conditions are satisfied. The quality of the coarse/surrogate model strongly affects the convergence of the SM optimization algorithm. Indeed, a poor coarse/surrogate model may result in a lack of convergence. To avoid this problem a method for assessing the quality of coarse/surrogate model is proposed in (Koziel *et al.* 2008).

To avoid the evaluation of the fine model several times and hence reduce computing time of SM technique a Space-Mapping-Based interpolation is proposed in (Koziel *et al.* 2006). The proposed interpolation scheme uses already available fine model data, so no additional fine model evaluations are necessary to perform this interpolation. The method sounds interesting but can't be used if there aren't fine model data as in case of new device design.

Manifold Mapping (MM) is a common SM technique that recently investigated in optimization of electromagnetic devices (Echeverria *et al.* 2006). An improvement of MM in terms of computing time and quality of optimal solution is studied in (Echeverria *et al.* 2007) by using a multilevel approach within the MM algorithm. Results show that three-level approach improved the quality of solution enclosed by MM but the gain on computing time is not significant. These results are found using two mathematical examples: Poisson-based optimization and a parameterized ellipse. In both examples coarse, medium and fine model are analytic and the optimization problem is without constraints. The three-level MM (3L-MM) algorithm is also applied in the optimization of an octangular double-layered shield in (Crevecoeur *et al.* 2009). An analytic model, a 2D and a 3D finite element models are used. 3L-MM converges towards satisfactory solution after 13 evaluations of the computationally expensive model.

Output Space Mapping (OSM) (Ben Ayed *et al.*, 2012) and (Encica *et al.*, 2008a) strategy is also an interesting variant of Space Mapping techniques. It aligns iteratively the fine model with the coarse model using correctors. This strategy is named two-level OSM (2L-OSM) because two models with different accuracy levels are used. The purpose of 2L-OSM is to achieve the optimization in a minimum evaluation number of the expensive model, and then it allows obtaining accurate results in a short computing time. However, the computing time of 2L-OSM can be significant because the fine model is evaluated one time at each iteration and

one fine model evaluation can take hours as in the case of 3D finite element model (3D FEM) (Tran *et al.*, 2010).

To overcome this problem, a generalized version of OSM strategy is proposed. The generalized algorithm is named n -Level Output Space Mapping (n L-OSM) technique and is able to take profit of n models of the device to optimize. The n models represent tradeoffs between accuracy of results and computation time.

This paper is structured in three main parts. Firstly, the conventional OSM algorithm is reminded. In the second part, the adapted n L-OSM technique is explained and detailed. The optimization benchmark problem of the Superconducting Magnetic Energy Storage (SMES) (Alotto *et al.*, 1996) is presented in the third part, as well as the models with different accuracy levels. Finally, the solutions and computation time of the 2L-OSM are compared to n L-OSM ones and some remarks on the use of the proposed algorithm are given in the conclusion.

II- OUTPUT SPACE MAPPING

Output Space Mapping (OSM) technique is a common approach for the optimization of devices represented by accurate, but time consuming, models. It has been recently used for solving optimization problems of electromagnetic converters (Encica *et al.*, 2008b) and (Tran *et al.*, 2009). This technique requires a second model, faster but less accurate, of the device to be optimally sized. This coarse model could be an empirical model, a FEM with a coarse mesh or an analytical model. The optimization is carried out with the coarse model and the results are validated with the fine one which is, in general, a high fidelity FEM.

The advantage of the OSM is its easier implementation. Indeed, by aligning the coarse model with the fine one, the precision is assured and the design space exploration is done by the optimization with the coarse model, avoiding though the possible numerical noise and mesh problems (Neittaanmäki *et al.*, 1996). The accuracy of optimization results are guaranteed by the FEM evaluations. Within the OSM technique, the role of the FEM is to adjust the analytical model outputs in order to better meet the constraints of the transformer optimization problem.

In a word, OSM is investigated in order to obtain satisfactory results with a minimum number of computationally expensive fine model evaluations. It aims to use both the coarse and fine models to reduce the computation time and increase the accuracy of the obtained solution.

III- n -LEVEL OUTPUT SPACE MAPPING TECHNIQUE

The proposed n L-OSM is expected to reduce even more the computational time compared to the conventional 2L-OSM. It takes advantages of the availability of n models of the device to optimize, each of them representing an optimal trade-off between the model error and its computation time. In Fig. 1, all the models are drawn as points which coordinates are the model error and the model computation time. The points belong to the Pareto optimal set and the curve joining those points is a Pareto front. The ideal model is the one that has the smallest error and time. Unfortunately, this model does not exist in reality. Fig. 1 shows that for an electromagnetic device it exists several models with different granularities. Each model presents an optimal trade-off between the model error and its computing time. The 1st model is the fastest while the n^{th} model is the most accurate.

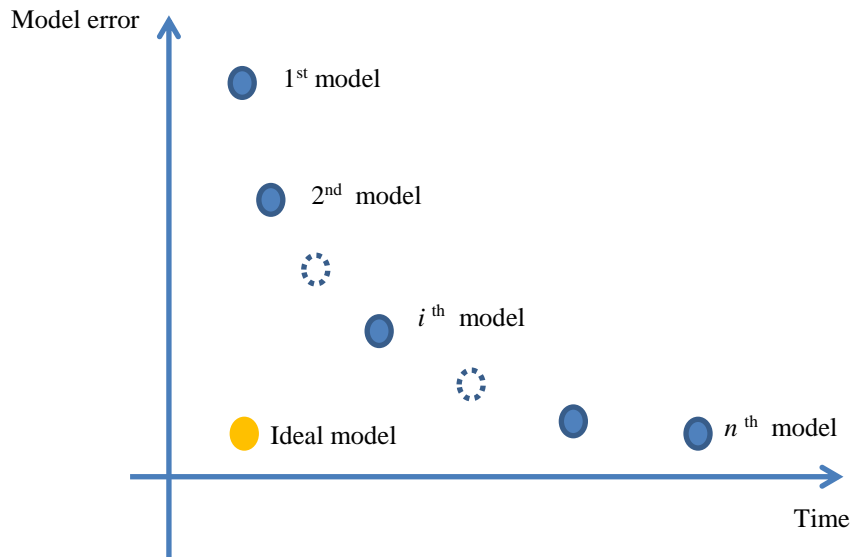


Figure 1. Models of the same electromagnetic device

The idea of the proposed algorithm is to use the 1st model during the optimization process to find an approximate solution. At iteration i , the i^{th} model is evaluated with this solution to update the correctors until the discrepancy between the corrected 1st model and the i^{th} model is small enough. The algorithm stops at iteration n when the corrected 1st model's outputs are equal to the n^{th} model's ones. Contrary to the classical 2L-OSM that use only the 1st and n^{th} models, the $n\text{L-OSM}$ uses all the n models to reduce the number of evaluations of the n^{th} model and thus the computation time.

In this paper, the coarse computationally cheaper model is denoted by $m_1(x) \in \mathbb{R}^p$ with $x \in \mathbb{R}^q$, the fine computationally expensive model is denoted by $m_n(x) \in \mathbb{R}^p$, and the $(n-2)$ models with k accuracy levels are denoted by $m_k(x) \in \mathbb{R}^p$, $k = 2..n-1$. The inputs of all models are the same. The nonlinear constraints of the coarse, k^{th} level accuracy, and fine models are $g_1(x)$, $g_k(x)$ and $g_n(x)$, respectively. Generally, the coarse model is denoted by $c(x)$ and the fine one is denoted by $f(x)$. In this paper $m_1(x)$ refers to $c(x)$ and $m_n(x)$ refers to $f(x)$. The optimization problem is expressed as:

$$(1) \quad x^* = \arg \min_{x \in X} \|m_n(x) - y\| \quad \text{s. t. } g_n(x) \leq 0$$

where $y \in \mathbb{R}^p$ denotes a vector of design specifications and can be zeros in the case of minimization. This problem is hard to solve and is decomposed into series of problems. The key point of OSM is to avoid the use of the fine model within the optimization process. So, as in the conventional OSM, the use of the fine model $m_n(x)$ within the optimization is avoided by using the coarse corrected model $m_1(x, \theta)$, where $\theta \in \mathbb{R}^p$ is the vector of correctors. The optimization problem at iteration j is:

$$(2) \quad x_j^* = \arg \min_{x \in X} \|m_1(x, \theta_1^j) - y\| \quad \text{s. t. } g_1(x, \theta_1^j) \leq 0$$

$$(3) \quad \begin{bmatrix} m_1(x, \theta_1^j) \\ g_1(x, \theta_1^j) \end{bmatrix} = \text{diag}(\theta_1^j) \cdot \begin{bmatrix} m_1(x) \\ g_1(x) \end{bmatrix}$$

The other problems consist of correcting the coarse model with a minimum evaluation number of the most accurate model. Then, to reach this goal, the strategy of the $n\text{L-OSM}$ is proposed. This strategy can be considered as a series of process that are launched iteratively. In the first process, the coarse model is corrected by the model with the next accuracy level (m_2) using the 2L-OSM algorithm. The others processes consist of aligning each model with the model that has the next level of accuracy. For example, during the k^{th} process, the k^{th} model is corrected by the $(k+1)^{\text{th}}$ model using corrective coefficients $\theta_k \in \mathbb{R}^p$. These coefficients are initialized to one and computed in order to have the same value for the outputs of the k^{th} and $(k+1)^{\text{th}}$ models.

$$(4) \quad \theta_1^{j+1} = \begin{bmatrix} m_2(x_j^*, \beta_2)/m_1(x_j^*) \\ g_2(x_j^*, \beta_2)/g_1(x_j^*) \end{bmatrix}$$

$$(5) \quad \beta_k = \begin{bmatrix} m_{k+1}(x_j^*, \beta_{k+1})/m_k(x_j^*) \\ g_{k+1}(x_j^*, \beta_{k+1})/g_k(x_j^*) \end{bmatrix} \quad k = 2..(n-1)$$

$$(6) \quad \begin{bmatrix} m_k(x_j^*, \beta_k) \\ g_k(x_j^*, \beta_k) \end{bmatrix} = \text{diag}(\beta_k) \cdot \begin{bmatrix} m_k(x_j^*) \\ g_k(x_j^*) \end{bmatrix} \quad k = 2..(n-1)$$

The space-mapping between the corrected coarse and 2^{nd} models stops when (7) is checked,

$$(7) \quad \left\| \begin{bmatrix} m_1(x_j^*, \theta_1^j) \\ g_1(x_j^*, \theta_1^j) \end{bmatrix} - \begin{bmatrix} m_2(x_j^*, \beta_k) \\ g_2(x_j^*, \beta_k) \end{bmatrix} \right\| \leq \varepsilon$$

If a solution is evaluated with a k^{th} model it cannot be evaluated with the next level $(k+1)$ model without checking (8),

$$(8) \quad \left\| \begin{bmatrix} m_1(x_j^*, \theta_1^j) \\ g_1(x_j^*, \theta_1^j) \end{bmatrix} - \begin{bmatrix} m_k(x_j^*, \beta_k) \\ g_k(x_j^*, \beta_k) \end{bmatrix} \right\| \leq \varepsilon$$

The $n\text{L-OSM}$ algorithm stops when (8) is checked and $k=n$. In (8), ε refers to the required accuracy of results. This stopping criterion affects strongly the number of loops within the SM algorithm as well as the evaluation number of the most consuming time model. In general, results are acceptable when the discrepancy between the fine and the coarse corrected model is equal or less than 10^{-4} .

To summarize, the nL -OSM algorithm carries out the following main steps:

- 0- initialization: $j = 0, k = 2, \theta_1^0 = I, \beta_{2..n} = I$
- 1- solve (2) in order to find x_j^* by using $m_1(x, \theta_1^j)$ as surrogate model
- 2- compute $m_2(x_j^*, \beta_2), g_2(x_j^*, \beta_2)$ and θ_1^{j+1} by using (4)
- 3- $j = j + 1$
- 4- go to step 1 until (7) is true
- 5- compute $m_{k+1}(x_j^*, \beta_{k+1})$ and $g_{k+1}(x_j^*, \beta_{k+1})$
- 6- compute $\beta_2 \cdots \beta_k$ by using (5)
- 7- go to step 1 until (8) is true
- 8- $k = k + 1$
- 9- go to step 5 while $k < n$
- 10- stop

IV- APPLICATION CASES

The application case is the optimization problem of a Superconducting Magnetic Energy Storage system (SMES) that is known as the team workshop problem #22.

The SMES device consists of two concentric superconducting coils fed with currents that flow in opposite directions. The system is used for storing magnetic energy with a minimum magnetic stray field over a square perimeter of 10 meters from coil axis (Team workshop, 1996) as shown in Fig. 3.

The optimal sizing problem consists of 3 design variables that are the radius (R_2), the width (d_2) and the height of the outer coils. The objectives of optimization are:

- The stored energy in the device should be 180 MJ.
- The magnetic field must not violate a physical condition (quench condition) which guarantees superconductivity.
- The stray field measured at 10 meters from the device should be as small as possible.

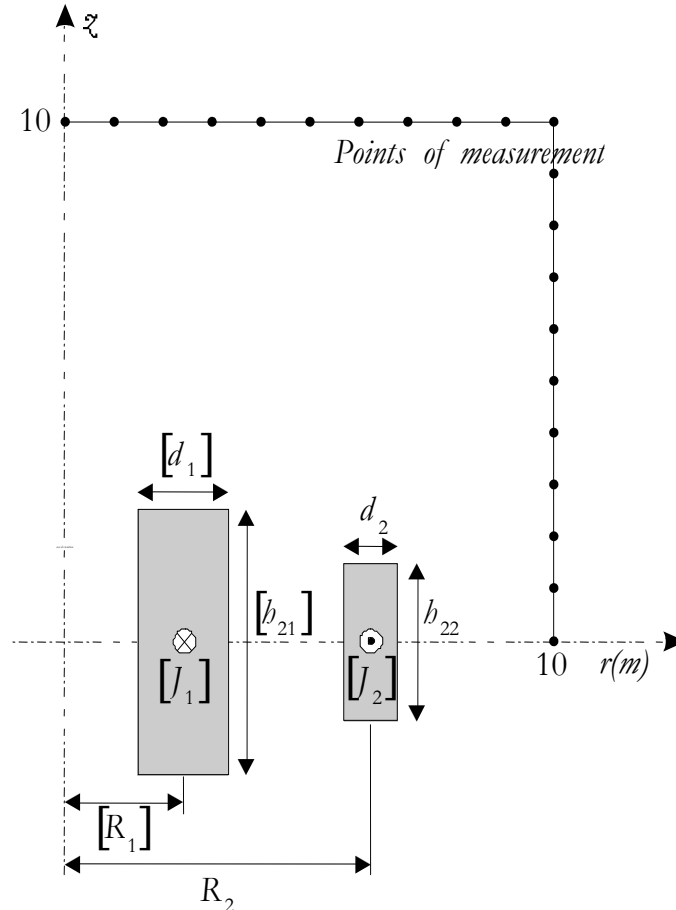


Figure 3. SMES design variables

1- 1st model

This model refers the coarsest model (m_1) within it, each coil of the device is considered as a single filamentary loop of radius a_i located at axis center (Rezzoug *et al.*, 1992). This approximation simplifies greatly the calculation of magnetic parameters and allows achieving acceptable results if the measurement point is far from the device (i.e. located at a distance $a_i \ll d$), else the discrepancy is great as well as the measurement point is near the device.

The mathematical expression of the vector potential A_i and both radial and axial components of the magnetic stray field $B_{\rho i}$, B_{zi} at the point P (x , y , z) are defined as follows (Wilson, 1983):

$$(9) \quad \text{Lets } \begin{cases} \rho = \sqrt{x^2 + y^2} \\ k_i = \sqrt{\frac{4a_i\rho}{(a_i+\rho)^2 + z_i^2}} \end{cases}$$

$$\begin{cases} A_i(\rho, z_i, I) = \frac{\mu_0 I}{k\pi} \sqrt{\frac{a_i}{\rho}} \left[\left(1 - \frac{k_i^2}{2}\right) K(k_i) - E(k_i) \right] \\ B_{\rho i}(\rho, z_i, I) = -\frac{\partial A}{\partial z} = \frac{\mu_0 I k_i z_i}{4\pi\rho\sqrt{a_i\rho}} \left[-K(k_i) + \frac{a_i^2 + \rho^2 + z_i^2}{(a_i - \rho)^2 + z_i^2} E(k_i) \right] \\ B_{zi}(\rho, z_i, I) = \frac{1}{\rho} \frac{\partial}{\partial \rho} (\rho A) = \frac{\mu_0 I k_i z_i}{4\pi\sqrt{a_i\rho}} \left[K(k_i) + \frac{a_i^2 - \rho^2 - z_i^2}{(a_i - \rho)^2 + z_i^2} E(k_i) \right] \end{cases}$$

where K and E are the complete elliptic integrals of the first and the second kinds, respectively. Then, the vector potential of the system can be deduced easily by adding A_1 and A_2 .

The stored energy by the two filamentary loops can be deduced from the mutual flux as follows:

$$(10) \quad \begin{cases} W_{e12} = \frac{1}{2} I_2 \Phi_{12} \\ \Phi_{12} = 2\pi a_2 A_1(\rho, (z_2 - z_1), I_1) \end{cases} \rightarrow W_{e12} = \pi a_2 I_2 \frac{\mu_0 I_1}{k\pi} \sqrt{\frac{a_1}{a_2}} \left[\left(1 - \frac{k^2}{2}\right) K(k) - E(k) \right]$$

where $k = \sqrt{\frac{4a_1 a_2}{(a_1 + a_2)^2 + (z_2 - z_1)^2}}$

2- k^{th} model

This model considers that each coil is made of N_k wires, carrying current $I = J \cdot dS$ as shown in Fig. 4. This approximation allows the calculation of different magnetic parameters at each point of the space with a small discrepancy (Rezzoug *et al.*, 1992).

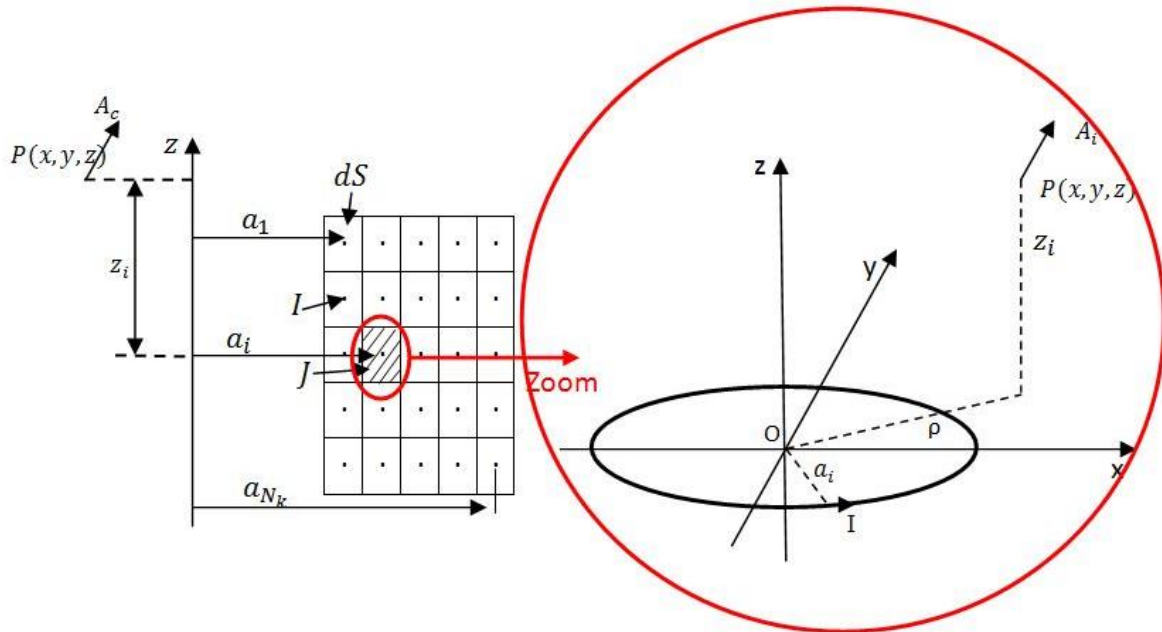


Figure. 4. Subdividing coil to filamentary loops

So, the vector potential A_c at P (x , y , z) generated by one coil and the stored energy W_c by the system can be written:

$$(11) \quad A_c(\rho, z_i, I) = \sum_{i=1}^{N_k} A_i(\rho, z_i, I) = \sum_{i=1}^{N_k} \frac{\mu_0 I}{k\pi} \sqrt{\frac{a_i}{\rho}} \left[\left(1 - \frac{k_i^2}{2}\right) K(k_i) - E(k_i) \right]$$

$$(12) \quad W_b = \sum_{i,j}^{i \neq j} W_{eij} = \sum_{i,j}^{i \neq j} \frac{1}{2} I_i \Phi_{ji}$$

With the same approach the magnetic stray field can be obtained easily.

3- n^{th} model

The n^{th} model has the highest accuracy. In our case it is a 2D FEM with fine mesh. It includes 552,202 nodes and 275,219 elements. One evaluation of this model takes 784 seconds.

4- Accuracy and computing time

The accuracy and computing time of the models increase with the number of filamentary loops used to model one coil. Therefore, many models with different levels of accuracy can be obtained easily by changing the number of loops as shown in Table 3. In this table, error refers the discrepancy between analytical models and 2D FEM outputs. Fig. 5 shows trade-offs between these models error and its computing time.

Table 3. Models accuracy and computation time

Type	Number of loops	Error (%)	Time (s)
m_1	1	254	0.016
m_2	100	7.2	1.61
m_3	400	0.3	24.8
m_4	900	0.14	127.53

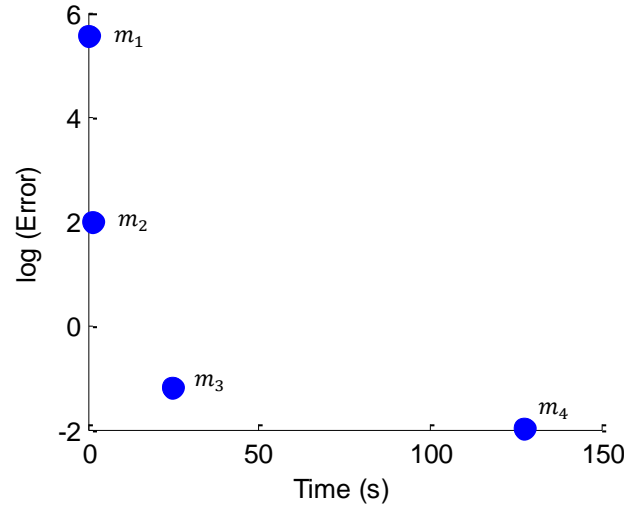


Figure. 5. Trade-offs between models error and computing time

Fig. 5 shows a Pareto front consisting trade-offs between models error and its computing time confirming that each model present an optimal compromise between error and time.

To justify the coherence of the analytical models, Fig 6 shows a comparison on calculated magnetic field within outer coil between an analytical model using 400 filamentary loops and the 2D FEM.

Fig. 6 shows through magnetic maps of the outer coil that the discrepancy between magnetic field values calculated by the medium model and the 2D FEM is less than 1%. This confirms the coherence of the analytical models built.

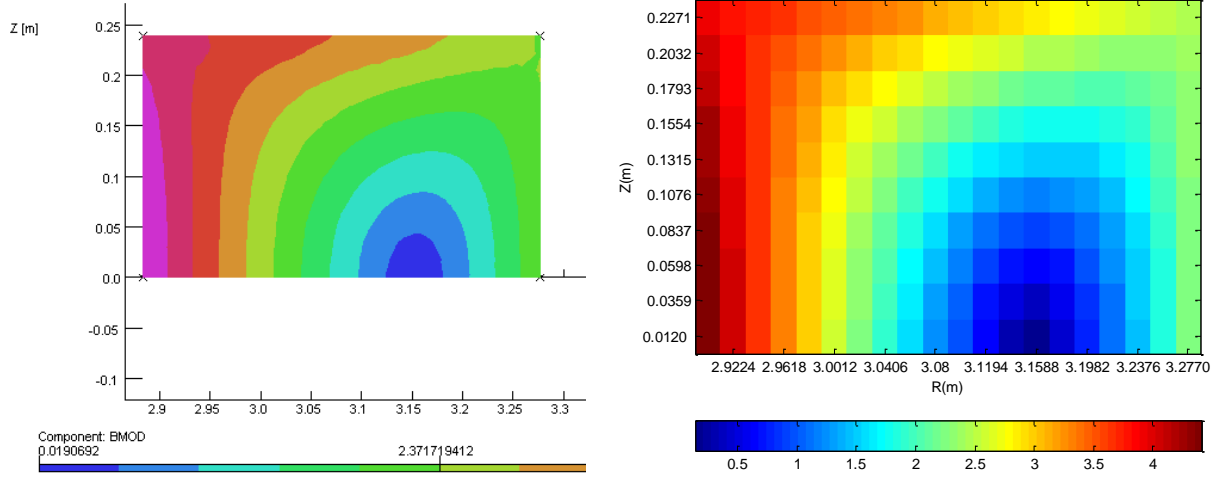


Figure. 6. Comparison between the analytical model using 400 filamentary loops (right) and a 2D FEM (left). Color code refers the flux density in Tesla. Axes refers to coils radial and central axis

5- Optimization problem

The goal of the optimization problem is to find the design configurations that give a specified value of stored magnetic energy and minimal magnetic stray field. Mathematically, this is formulated as:

$$(14) \quad \min_{R_2, h_2, d_2} OF = \frac{B_{stray}^2}{B_{norm}^2} + \frac{|Energy - E_{ref}|}{E_{ref}}$$

$$with \quad \begin{cases} 2.6 \text{ m} \leq R_2 \leq 3.4 \text{ m} \\ 0.204 \text{ m} \leq h_2/2 \leq 1.1 \text{ m} \\ 0.1 \text{ m} \leq d_2 \leq 0.4 \text{ m} \end{cases}$$

$$s.t. |J_2| \leq (-6.4|B| + 54)A/mm^2$$

where $B_{stray}^2 = \frac{\sum_{i=1}^{22} |B_{stray_i}|^2}{22}$; $E_{ref} = 180 \text{ MJ}$ and $B_{norm} = 3 \text{ mT}$ with B_{stray_i} is the magnetic field measured in one point (i) located at 10 meters from the device.

6- Optimization results

In order to minimize the risk to enclose local optimum, optimization with the surrogate analytical model is launched with 10 starts points. The optimization uses Sequential Quadratic Programming (SQP) method that allows obtaining an optimum in a very short time.

Table 4 and 5 shows the results obtained with different number of models. Table 4 shows the computation time and the number of evaluations of each SMES model. Table 5 shows a comparison between optimal solutions found by the nL -OSM algorithm and an optimum solution found in literature (Team workshop, 1996).

Table 4. Computation time and evaluation number of each SMES model

Evaluation number of each model	m_5	m_4	m_3	m_2	m_1	Time (s)
5L-OSM	2	2	2	10	1225	1849
4L-OSM	2	2	3	-	1230	1849
3L-OSM	2	4	-	-	1452	2101
2L-OSM	7	-	-	-	2476	5527

Table 5. Optimum found by different algorithms

	R_2 (m)	$h_2/2$ (m)	d_2 (m)	OF	B_{stray}^2 (T ²)	Energy (MJ)
(Team workshop, 1996)	3.08	0.2390	0.3940	0.08808	7.9138e-7	180.0277
2L-OSM	3.08	0.2405	0.3937	0.08910	7.9382e-7	180.1622
3L-OSM	3.08	0.2405	0.3937	0.08920	7.9530e-7	180.1572
4L-OSM	3.08	0.2405	0.3936	0.08960	7.9503e-7	180.2215
5L-OSM	3.08	0.2405	0.3936	0.08963	7.9501e-7	180.2535

n -level OSM algorithm and the global optimization algorithm used in (Team workshop, 1996) converge to the same solution. This confirms that multi-starts optimization is an efficient method to reduce the risk of local optimum when using a local optimization algorithm such as SQP.

The 2-level OSM and the n -level OSM algorithms converge to the same solution. However, the computation time has decrease up to 3 times, thanks to the addition of models with intermediate accuracy and computation time. The computation time of n L-OSM stop to decrease when the number of intermediate models is greater than 2 in the case of the SMES. Indeed, computing time of the 5L-OSM and 4L-OSM are equal.

In the case of the SMES, the 4L-OSM is the best algorithm in terms of computing time. This result can't be generalized to other cases because the efficiency in terms of computing time of the n L-OSM is forcefully related to the accuracy and the computing time of built coarse and medium models. It's very important to highlight that it is possible that the computing time of the n L-OSM algorithm can be greater than the $(n-1)$ L-OSM if medium models are chosen incorrectly: first feelings through the SMES case show that to have an additional gain on computing time, the introduced medium model (k) must satisfy two conditions. The first one is the medium model (k) must be at least three-times more accurate and ten-times less rapid than the coarse model. The second condition is that the medium model k must be at least seven-times more rapid and three-times less accurate than the medium model ($k+1$).

V-CONCLUSION

The n -level OSM algorithm allows reducing computing time in comparison with the traditional OSM algorithm thanks to $n-2$ models inserted between the coarse and the fine model. Inserted models can be obtained easily by changing the mesh size in FEM, the number of elements in lumped-mass models, and the number of assumptions in analytical models.

Using the different models with different granularities, the n -level OSM algorithm converge to the same optimum found by the conventional OSM algorithm with a major reduction of computing time equals to 3 and without decreasing the performance of the space mapping technique.

The gain in computing time with the adapted space mapping algorithm stops increasing when number of medium models is important. To avoid meeting this case, the authors propose to search for an automatic diagnostic of models to find the optimal number of medium models to introduce between coarse and fine ones.

VI- REFERENCES

- Alotto, P., Kuntsevitch, A.V., Magele, C., Molinari, G., Paul, C., Preis, K., Repetto, M., Richter, K.R., (1996), "Multiobjective optimization in magnetostatics: a proposal for benchmark problems", *IEEE transactions on magnetics*, Vol. 32, No 3, pp. 1238-1241.
- Bandler, J.W, Biernacki, R.M, Chen, S.H., Grobelny, P.A, and Hemmers, R.H., (1994), "Space mapping technique for electromagnetic optimization", *IEEE transactions on microwave theory and techniques*, Vol. 42, No. 12, pp. 2536-2544.
- Ben Ayed, R., Brisset, S., (2012) "Multidisciplinary optimization formulations benefits on space mapping techniques", *The international journal for computation and mathematics in electrical and electronic engineering (COMPEL)*, vol. 31, no. 3, pp. 945-957.
- Crevecœur, G., Sergeant, P., Dupré, L., and Van de Walle, R., (2009), "Optimization of an octangular double-layered shield using multiple forward models", *IEEE transactions on magnetics*, Vol. 45, No. 3, pp. 1586-1589.
- Echeverria, D., Lahaye, D., Encica L., and Hemker, P.W., (2005), "Optimization in electromagnetic with the space mapping technique". *The international journal for the computation and mathematics in electrical and electronic engineering (COMPEL)*, vol. 24, no. 3, pp.952-966.
- Echeverria, D., Lahaye, D., Encica, L., Lomonova, E.A., Hemker, P.W., and Vandenput, A.J.A., (2006), "Manifold-Mapping optimization applied to linear actuator design", *IEEE transactions on magnetics*, Vol. 42, No. 4, pp. 1183-1186.
- Echeverria, D., (2007), "Multi-level optimization: Space Mapping and Manifold Mapping", Ph.D. thesis available at <http://pangea.stanford.edu/~echeverr/smpapers/tesis00.pdf>.
- Encica, L., Paulides, J.J.H., Lomonova, E.A., and Vandenput, A.J.A., (2008a), "Aggressive output space-mapping optimization for electromagnetic actuators", *IEEE transactions on magnetics*, Vol. 44, No. 6, pp. 1106-1109.
- Encica, L., Paulides, J.J.H., Lomanova, E.A., and Vandenput, A.J.A., (2008b), "Electromagnetic and thermal design of a linear actuator using output polynomial space mapping", *IEEE transactions on industry applications*, Vol. 44, No. 2, pp. 534-542.
- Koziel, S., Bandler, J.W., Madsen, K., (2006), "Space-Mapping-Based interpolation for engineering optimization", *IEEE transactions on microwave theory and techniques*, Vol. 54, No. 6, pp. 2410-2421.
- Koziel, S., Bandler, J.W., Madsen, K., (2008), "Quality assessment of coarse models and surrogates for space mapping optimization", *optimization and engineering journal*, springer, issue 9, pp. 375-391.
- Neittaanmäki, P., Rudnicki, M., and Savini, A., (1996), *Inverse problems and optimal design in electricity and magnetism*, Oxford University Press Inc., New York, pp. 325-348.
- Rezzoug, A., Caron, J.P., Sargos, M., (1992), "Analytical calculations of flux induction and forces of thick coils with finite length", *IEEE transactions on magnetics*, vol. 28, no. 5.

Team workshop problem 22. (1996), available at: http://www.igte.tugraz.at/archive/team_new/team3_res.php

Tran, T.V., Brisset, S., and Brochet, P., (2009), "A New efficient method for global discrete multilevel optimization combining branch-and-bound and space mapping". IEEE transaction on magnetics, Vol. 45, No. 3, pp. 1590-1593.

Tran, T.V., Moussini, F., Brisset, S., and Brochet, P., (2010), "Adapted Output Space-Mapping Technique for a Bi-Objective Optimization", IEEE Transactions on Magnetism, vol. 46, no. 8, pp. 2990-2993.

Wilson, M.N., Superconducting Magnets, Oxford Science Publications, 1983.